Contents lists available at SciVerse ScienceDirect

Computational and Theoretical Chemistry

M(C₆X₆Li₆)₂ (M = Cr, Mo, W; X = O, S): Transition-metal sandwich complexes with π-aromatic C₆X₆Li₆ ligands

Jin-Chang Guo, Hai-Gang Lu *, Si-Dian Li *

Institute of Molecular Science, Shanxi University, Taiyuan 030001, Shanxi, PR China

ABSTRACT

The geometrical and electronic structures of a new class of transition-metal sandwich complexes M(C₆X₆Li₆)₂ (M = Cr, Mo, W; X = O, S) have been systematically investigated in this work at DFT B3LYP and PBE1PBE levels. Both the D_{2d} M(C₆O₆Li₆)₂ and D_{6d} M(C₆S₆Li₆)₂ (M = Cr, Mo, W) complex series are found to conform to the 18-electron rule similar to dibenzenechromium Cr(C₆H₆)₂ and are stable in thermodynamics. Molecular orbital analyses indicate that effective d–π coordination bonds are formed between the partially filled nd atomic orbitals of transition-metal centers (Cr, Mo, W) and the π molecular orbitals of the C₆X₆Li₆ ligands (X = O, S). Electrostatic interactions between the two interlaced C₆X₆Li₆ (X = O and S) ligands also contribute to the high stability of these sandwich complexes. The calculated infrared spectra of these complexes are presented to facilitate their future experimental characterizations.

Crown Copyright © 2013 Published by Elsevier B.V. All rights reserved.

1. Introduction

Since the discovery of ferrocene Fe(C₅H₅)₂ [1,2] and dibenzenechromium Cr(C₆H₆)₂ [3], transition-metal sandwich complexes have constituted one of the most important subjects in organometallic chemistry. The interesting geometrical, electronic structures and unusual bonding characteristics of these sandwich complexes have attracted great attention because of their wide applications in catalysis, polymers, and molecular recognitions [4]. Typical such complexes possess a mononuclear M center sandwiched between two small carbocyclic ligands [5–7]. The d–π interactions between the transition metal centers and their ligands play a key role in stabilizing these sandwich structures. To improve the properties of sandwich complexes, chemists have been managing to modify and design new ligands in the past six decades. A number of novel ligands analogous to benzene have been designed to sandwich transition mental center in recent years, such as B₆C²⁻, P₅⁻, C₆₀ [8–13]. These novel sandwich complexes, ions, multidecker sandwich clusters and infinitely long sandwich complexes (or nanowires) with unusual structures and chemical properties have helped to understand the nature of the d–π coordination interactions [14–20].

In order to reduce greenhouse gas emissions, carbonyl (CO)-based molecules have aroused great interest among chemists in recent years [21–29]. When benzenehexol (C₆O₆H₆) [30] and benzenehexathiol (C₆S₆H₆) [31] lose six H⁺ cations from the

hydroxyl and hydrosulfuryl groups, the hexaanions of $C_6O_6^{6-}$ and $C_6S_6^{6-}$ are formed. The salts of $C_6O_6^{6-}$ and $C_6S_6^{6-}$ have found wide applications [32,33]. Hexasodium hexathiolate C₆S₆Na₆ has been synthesized experimentally and its X-ray crystal structure has been determined [31,34]. The perfect molecular wheels of C₆O₆Li₆ and C₆S₆Li₆ turn out to be the true minima of the systems, with the six lithium cations at bridging positions. The C₆O₆Li₆–C₆O₆Li₄ pair has found potential application in Li⁺-battery [35]. Similar to benzene (D_{6h} C₆H₆), the perfect "molecular wheels" of D_{6h} C₆O₆Li₆ and C₆S₆Li₆ appear to be π-aromatic in nature with six delocalized π electrons conforming to the $4n + 2$ Huckel rule (see Fig. 1) and therefore are possible to serve as alternative ligands to coordinate transition metal centers. Recently, Eiji Asato et al. reported the novel mixed-valence heptanuclear palladium complex of [Pd₇(THBQ)₂(tben)₆](PF₆)₄ in which two C₆O₆ units show an unprecedented η⁶–C₆O₆ binding mode to a naked Pd metal. Such a structure is reminiscent of the typical metallocene-like compounds [36]. Wu and co-workers recently predicted that crystallized M(C₆O₆H₆)ₙ sandwich nanowires may serve as ferroelectric or even multiferroic materials [37].

However, to the best of our knowledge, there have been no experimental or theoretical investigations reported to date on transition-metal sandwich complexes containing the π-aromatic C₆X₆Li₆ (X = O, S) ligands. We aim in this work to explore at density functional theory (DFT) level the geometrical and electronic structures, aromaticities, and thermodynamic stabilities of a series of novel sandwich complexes M(C₆X₆Li₆)₂ (M = Cr, Mo, W; X = O, S) in which the transition metal center M are effectively sandwiched between two π-aromatic C₆X₆Li₆ ligands. Such structures which may be generated through ligand exchange reactions from

* Corresponding authors.
   E-mail addresses: haigang_lu@yahoo.com.cn (H.-G. Lu), lisidian@yahoo.com (S.-D. Li).
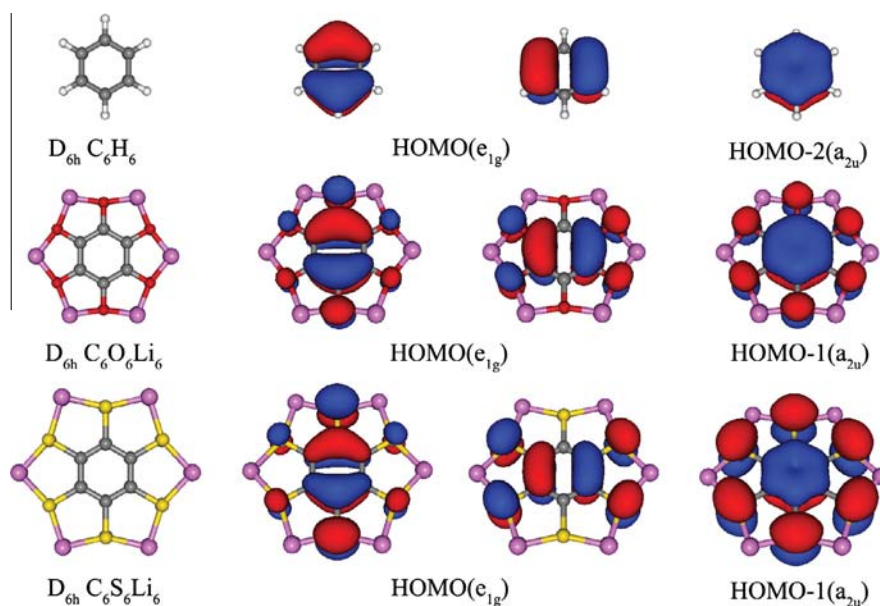
Fig. 1. Geometrical structures of D_{6h} C_6H_6, $C_6O_6Li_6$, and $C_6S_6Li_6$ and their delocalized orbitals obtained at B3LYP.

dibenzenechromium $Cr(C_6H_6)_2$ extend the structural domain of transition-metal sandwich complexes and may have important applications in chemistry and materials science.

2. Theoretical methods

The geometrical optimizations were performed using the hybrid B3LYP [38,39] and PBE1PBE [40] with the standard Gaussian basis of 6-311+G(d) on H, C, O, S, Li, Cr and the Stuttgart quasi-relativistic pseudo-potentials and basis sets (Stuttgart RSC 1997 ECP) augmented with 2f and 1 g functions on Mo and W [41–43]. Geometries were fully optimized and the DFT wave functions obtained at the optimized structures were confirmed to be stable. Vibrational frequencies of the optimized structures at the same levels were calculated to characterize stationary points as minima, transition states, or high-order saddle points on the potential energy surfaces (PES). Natural bond orbital (NBO) analyses were performed to gain insight into the bonding pattern of these complexes. Because all the transitional-metal centers in these complexes conform to the 18-elececton rule similar to the situation in $Cr(C_6H_6)_2$, the ground states of these sandwich complexes appear to be singlet. To assess the aromatic character of these sandwich complexes, the nucleus independent chemical shifts (NICS) and their out-of-plane components ($NICS_{zz}$) [44–47] were calculated at points 1.0 Å above the C_6-ring centers along the molecular axes perpendicular to the ligand planes. All DFT calculations in this work were carried out using the Gaussian 03 package [48]. Molecular structures and Molecular orbitals were visualized using the CYLview [49] and Molekel 5.4 [50] program, respectively.

3. Results and discussion

3.1. Geometrical structures

Fig. 2 depicts the optimized structures of the sandwich complexes $M(C_6X_6Li_6)_2$(M = Cr, Mo, W; X = O, S) at B3LYP. The PBE1PBE functional produces essentially the same structures for these complexes, with only minor differences in bond lengths.

In the following discussions, we will mainly investigate the geometrical and electronic properties of the concerned complexes using the B3LYP functional. Similar to the classical sandwich structure of $Cr(C_6H_6)_2$, the metal center M form sandwich structures with two staggered C_6 rings in both the $M(C_6O_6Li_6)_2$ and $M(C_6S_6Li_6)_2$ series (M = Cr, Mo, W). The Cr–C bond lengths of 2.105–2.195 Å in $Cr(C_6O_6Li_6)_2$ and 2.182 Å in $Cr(C_6S_6Li_6)_2$ are very close to the corresponding values of 2.171 Å in $Cr(C_6H_6)_2$, indicating that the $M(C_6X_6Li_6)_2$ molecules concerned in this work belong to typical transitional-metal sandwich complexes.

However, the staggered $M(C_6X_6Li_6)_2$ appear to be also obviously different from the eclipsed $Cr(C_6H_6)_2$ in structural features which are obviously related with the $C_6X_6Li_6$ ligands they contain. The $M(C_6S_6Li_6)_2$ series form perfect staggered D_{6d} geometric structures (see Fig. 2) due to the electrostatic interactions between the two ligands in the complexes. As shown in Table 1, S and Li atoms carry the natural atomic charges of −0.58 to −0.59 |e| and +0.77 |e|, respectively. An eclipsed D_{6h} structure is therefore expected to be unstable due to the obvious electrostatic repulsion between the S and Li atoms in the two ligands at the two ends. In fact, as shown in Fig. S1, the eclipsed D_{6h} $Cr(C_6S_6Li_6)_2$ is an eighth-order saddle point lying much higher in energy (3.31 eV) than the perfectly staggered D_{6d} geometry. Such staggered D_{6d} conformations help to form effective electrostatic attraction between the neighboring S and Li ions in the two opposite ligands, leading to the interlaced cage-like structures for the whole D_{6d} $M(C_6S_6Li_6)_2$ series (M = Cr, Mo, W). However, as O is smaller than S in atomic radii and $C_6O_6Li_6$ is smaller than $C_6S_6Li_6$ in ligand sizes, there would be no enough space to place the twelve Li^+ ions in the perfectly staggered D_{6d} $M(C_6O_6Li_6)_2$. It is true that, in the case of $Cr(C_6O_6Li_6)_2$, the perfectly eclipsed D_{6h} (a transition state), the perfectly staggered D_{6d} (a ninth-order saddle point), and the slightly distorted D_3 (a true minimum) structures lie 2.64, 1.31, and 0.27 eV higher than the lowest-lying D_{2d} isomer obtained, respectively. Four Li ions are eventually excluded from the middle part of the staggered $Cr(C_6O_6Li_6)_2$ to form the slightly distorted D_{2d} $Cr(C_6O_6Li_6)_2$ which contain four Li^+ cations 0.54 Å above the ligand planes. Similar D_{2d} distortion occur to other $M(C_6O_6Li_6)_2$ complexes.

3.2. Bonding characteristics

The bonding characteristics of these sandwich complexes also appear to be interesting. As shown in Table 1, the natural atomic charges of carbon atoms in $C_6O_6Li_6$ are slightly positive (+0.17), while those in C_6H_6 and $C_6S_6Li_6$ are negative (−0.21 and −0.17).
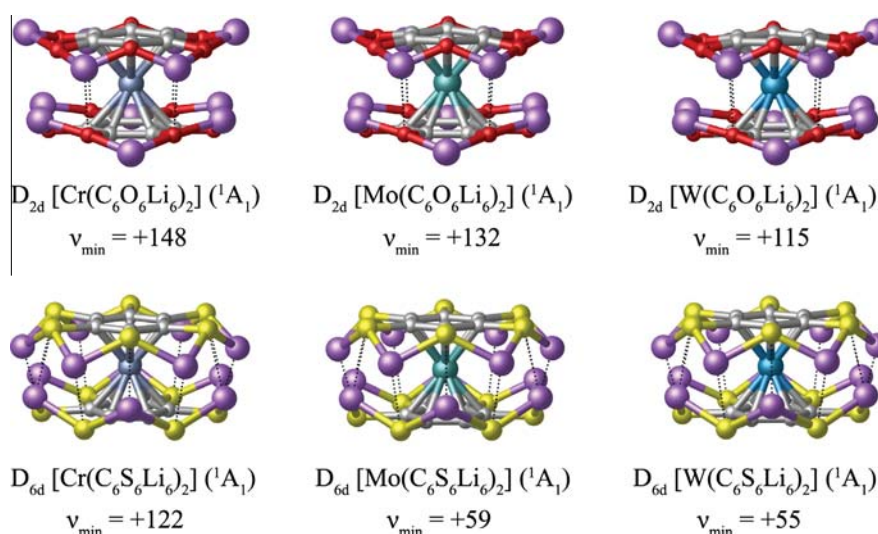
Fig. 2. Optimized structures of the sandwich complexes D_{2d} $M(C_6O_6Li_6)_2$ and D_{6d} $M(C_6S_6Li_6)_2$ (M = Cr, Mo, W) at B3LYP.

Table 1
Calculated bond lengths (r/Å), natural atomic charges (q/|e|) of C_6H_6, $C_6X_6Li_6$, $[Cr(C_6H_6)_2]$, and $[M(C_6X_6Li_6)_2]$ (M = Cr, Mo, W; X = O, S) at B3LYP.

	r_{C-M}	r_{C-C}	r_{C-X}	r_{X-Li}	r_{Li-Li}	q_M	q_C	q_X	q_{Li}
C_6H_6		1.395	1.084				−0.21	+0.21	
$C_6O_6Li_6$		1.409	1.388	1.781			+0.17	−1.11	+0.94
$C_6S_6Li_6$		1.418	1.808	2.193			−0.17	−0.71	+0.88
$Cr(C_6H_6)_2$	2.171	1.416	1.084			−0.02	−0.22	+0.22	
$Cr(C_6O_6Li_6)_2$	2.195	1.443	1.357	1.800	2.342	−0.65	+0.28	−0.93	+0.76
	2.105	1.445	1.407	1.832			+0.21	−0.99	+0.86
				1.950					
$Mo(C_6O_6Li_6)$	2.298	1.457	1.357	1.817	2.328	−0.78	+0.28	−0.92	+0.76
	2.213	1.458	1.406	1.836			+0.21	−0.98	+0.86
				1.972					
$W(C_6O_6Li_6)_2$	2.305	1.459	1.357	1.819	2.336	−0.61	+0.29	−0.92	+0.73
	2.220	1.459	1.408	1.839			+0.22	−0.97	+0.84
				1.977					
$Cr(C_6S_6Li_6)_2$	2.182	1.443	1.841	2.239	2.542	−0.03	−0.18	−0.59	+0.77
$Mo(C_6S_6Li_6)_2$	2.269	1.452	1.844	2.243	2.560	−0.12	−0.18	−0.58	+0.77
$W(C_6S_6Li_6)_2$	2.276	1.456	1.846	2.244	2.568	+0.12	−0.20	−0.58	+0.77

Therefore, $C_6O_6Li_6$ is expected to be different from C_6H_6, and $C_6S_6Li_6$ is anticipated to be similar with C_6H_6. It is true that, in the sandwich complexes, the metals and carbon atoms in $M(C_6O_6Li_6)_2$ are negatively and positively charged, respectively, while the metal and carbon atoms in both $Cr(C_6H_6)_2$ and $M(C_6S_6Li_6)_2$ are positively and negatively charged, respectively. We employ the widely used Wiberg bond index to investigate the coordination bonding in these complexes. As shown in Table 2, the total Wiberg bond order of $Cr-C_{12}$ in $Cr(C_6O_6Li_6)_2$ (4.79) is obviously higher than those in $Cr(C_6H_6)_2$ (3.91) and $Cr(C_6S_6Li_6)_2$ (3.80). Similarly, the total bond orders in $Mo(C_6O_6Li_6)_2$ and $W(C_6O_6Li_6)_2$ are higher than those in $Mo(C_6S_6Li_6)_2$ and $W(C_6S_6Li_6)_2$, respectively. These results indicate that the $Cr-C_{12}$ coordination interaction for $C_6O_6Li_6$ ligand is stronger than that for both $C_6S_6Li_6$ and C_6H_6. The higher $M-C_{12}$ bond orders in $M(C_6O_6Li_6)_2$ are consistent with the negative charges the metal centers carry in $M(C_6O_6Li_6)_2$ complexes. Such charge distributions originate from effective d–π donations and provide more bonding nd electrons for the metal centers to coordinate with its $C_6S_6Li_6$ ligands. Detailed NBO analyses indicate that there are minor bonding contributions between the metal center and the O_{12}/S_{12} lone pairs as well, with the total Wiberg bond orders of about 0.49–0.63 (see Table 2). Thus, the ligands in $M(C_6O_6Li_6)_2$ are coordinated with the metal center not only through the C_6 aromatic rings, but also through the O/S lone pairs. We also notice that

the Cr center in $Cr(C_6S_6Li_6)_2$ has the atomic electronic configuration of $Cr[Ar]4s^{0.01}3d^{5.72}$, indicating that the 4s electron is almost completely lost in the Cr center. In this electronic configuration, Cr center would mainly coordinates with its ligands through $3d$ orbitals. Other $M(C_6X_6Li_6)_2$ sandwich complexes have similar situations.

The NICS and $NICS_{zz}$ values of the $C_6X_6Li_6$ ligands and $M(C_6X_6Li_6)_2$ complexes (M = Cr, Mo, W; X = O, S) at points 1.0 Å above the ring center of the C_6 ligands along the molecular axes are computed at GIAO-B3LYP (see Table 2). The calculated NICS(1) (−10.4 and −8.4 ppm) and $NICS_{zz}(1)$(−21.2 and −20.2 ppm) for D_{6h} $C_6O_6Li_6$ and $C_6S_6Li_6$ appear to be well comparable with the corresponding values of C_6H_6 (−10.0 and −29.4 ppm), indicating that the $C_6X_6Li_6$ (X = O, S) ligands possess similar π-aromaticity with C_6H_6. It is worth noticing that the calculated negative NICS(1) (−14.1 to −19.3 ppm) and $NICS_{zz}(1)$ (−22.8 to −25.4 ppm) values for the sandwich complexes appear to be even bigger than the corresponding value of free $C_6X_6Li_6$ ligands, indicating that the nd_{z2} orbitals of the transition-metal centers also contribute to the overall aromaticity of the ligands in the complexes.

The stability of $M(C_6X_6Li_6)_2$ (M = Cr, Mo, W; X = O, S) complexes mainly originate from their bonding patterns involving effective interactions between the partially filled nd orbitals of the transition-metal centers M and the delocalized π orbitals of the

Table 2
Wiberg bond indices (WBI), NICS(1) and NICS$_{zz}$(1) and HOMO–LUMO energy gaps (ΔE_{gap}/eV) of C_6H_6, $C_6X_6Li_6$, $Cr(C_6H_6)_2$, and $M(C_6X_6Li_6)_2$ (M = Cr, Mo, W; X = O, S) at B3LYP.

	WBI					NICS (1)	NICS$_{zz}$(1)	ΔE_{gap}
	M–C$_{12}$	M–X$_{12}$	C–C	C–X	X–Li			
C_6H_6			1.44	0.93		−10.0	−29.4	6.60
$C_6O_6Li_6$			1.31	1.03	0.05	−10.4	−21.2	2.16
$C_6S_6Li_6$			1.34	1.06	0.11	−8.4	−20.2	2.99
$Cr(C_6H_6)_2$	3.91	0.16	1.28	0.91		−20.1	−34.7	4.00
$Cr(C_6O_6Li_6)_2$	4.79	0.49	1.12	1.08	0.10	−19.3	−22.8	1.83
			1.12	0.99	0.13			
$Mo(C_6O_6Li_6)$	4.43	0.63	1.12	1.09	0.13	−15.5	−23.4	2.19
			1.12	1.00	0.09			
$W(C_6O_6Li_6)_2$	4.74	0.56	1.11	1.07	0.15	−15.8	−25.0	2.20
			1.12	0.98	0.12			
$Cr(C_6S_6Li_6)_2$	3.80	0.62	1.21	1.02	0.12	−17.3	−23.0	2.56
$Mo(C_6S_6Li_6)_2$	4.13	0.62	1.19	1.02	0.12	−14.2	−25.4	2.46
$W(C_6S_6Li_6)_2$	4.33	0.60	1.18	1.02	0.12	−14.1	−22.9	2.39
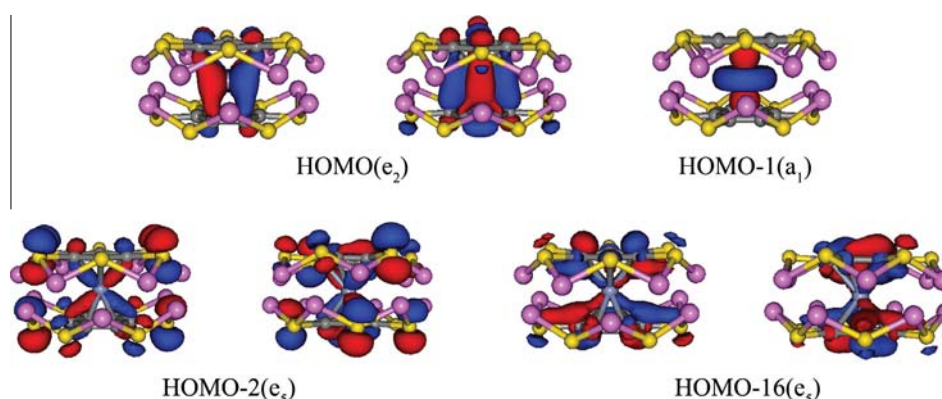
Fig. 3. MO pictures of D$_{6d}$ Cr(C$_6$S$_6$Li$_6$)$_2$ at B3LYP involving the Cr 3d orbitals and the π orbitals of the two C$_6$S$_6$Li$_6$ ligands.

C$_6$X$_6$Li$_6$ ligands. We illustrate the bonding molecular orbitals of the high symmetry D$_{6d}$ Cr(C$_6$S$_6$Li$_6$)$_2$ in Fig. 3 which involve the 3d orbitals of the Cr center and the π orbitals of C$_6$S$_6$Li$_6$ ligand. The degenerate HOMOs(e$_2$) of Cr(C$_6$S$_6$Li$_6$)$_2$ are the combination of the 3d$_{xy}$ and 3d$_{x2-y2}$ orbitals of the Cr center with the degenerate antibonding ππ* MOs of the C$_6$S$_6$Li$_6$ ligand which makes the largest contribution to Cr(C$_6$S$_6$Li$_6$)$_2$ δ-back-donation. The HOMO-1(a$_1$) mainly originates from the 3d$_{z2}$ atomic orbital of Cr atom. HOMO-2(e$_5$) reflects the interactions between the two π HOMOs (e$_{1g}$) of the two C$_6$S$_6$Li$_6$ ligands with opposite orbital signs and the 3d$_{xz}$ and 3d$_{yz}$ of the Cr center, which mainly contain the electron donation from the C$_6$S$_6$Li$_6$ ligands to the 3d$_{xz}$ and 3d$_{yz}$ atomic orbitals of the Cr atom. It is interesting to notice that HOMO-16(e$_5$) also contain the contributions from the lone pair orbitals of S atoms. Similar d–π bonding MOs exist in the other M(C$_6$X$_6$Li$_6$)$_2$ sandwich complexes. It is these effective d–π interactions including the LM donation and ML back-donation that play the most important roles in maintaining the stabilities of M(C$_6$X$_6$Li$_6$)$_2$ (M = Cr, Mo, W; X = O, S) complexes.

3.3. Thermodynamic stabilities and Simulated IR Spectra

Concerning the thermodynamic stabilities of these novel sandwich complexes, we propose the following C$_6$X$_6$Li$_6$/C$_6$H$_6$ ligand exchange reactions in gas phases in The reactions of D$_{6h}$ C$_6$X$_6$Li$_6$ ligands with D$_{6h}$ M(C$_6$H$_6$)$_2$ to produce M(C$_6$X$_6$Li$_6$)$_2$ (M = Cr, Mo, W; X = O, S) and free C$_6$H$_6$ can be divided into two steps: (1) and (2). As indicated in Table 3, with zero-point corrections included, the overall reactions all have the negative total energy changes of E = ΔE_1 + ΔE_2 (−11.61 to −44.83 kcal/mol) at the B3LYP level,

indicating that the replacements of C$_6$H$_6$ ligands in D$_{6h}$ M(C$_6$H$_6$)$_2$ with D$_{6h}$ C$_6$X$_6$Li$_6$ are overall favored in energy. Interestingly, the first step reaction (R.1) possesses small positive energy changes with ΔE_1 = +1.14 to +3.89 kcal/mol for C$_6$S$_6$Li$_6$ and the small negative energy changes with ΔE_1 = −2.72 to −9.16 kcal/mol for C$_6$O$_6$Li$_6$. These values suggest that the formation of the mixed sandwich complexes M(C$_6$X$_6$Li$_6$)(C$_6$H$_6$) may be reversible processes. However, such reversible processes can be effectively coupled with the second step reactions which are overwhelmingly favored in thermodynamics with much bigger negative energy changes, making the overall reactions favorable in thermodynamics (see Table 3). Based upon this observation, we propose the possibility of synthesizing the concerned sandwich complexes through ligand exchange reactions in gas phases.

In addition, as shown in Table 2, all these sandwich complexes possess relatively large HOMO–LUMO energy gaps with ΔE_{gap} = 1.83–2.56 eV, further supporting their thermodynamic stability. Detailed kinetic investigation on such big complexes

Table 3
Calculated energy changes ΔE (kcal/mol) for Reaction 1 and Reaction 2 at B3LYP with zero-point corrections included.

	ΔE_1	ΔE_2	$\Delta E_1 + \Delta E_2$
$Cr(C_6O_6Li_6)_2$	−2.72	−33.15	−35.87
$Mo(C_6O_6Li_6)_2$	−8.21	−4.54	−12.75
$W(C_6O_6Li_6)_2$	−9.16	−2.45	−11.61
$Cr(C_6S_6Li_6)_2$	+3.89	−43.81	−39.92
$Mo(C_6S_6Li_6)_2$	+1.52	−45.36	−43.84
$W(C_6S_6Li_6)_2$	+1.14	−45.97	−44.83
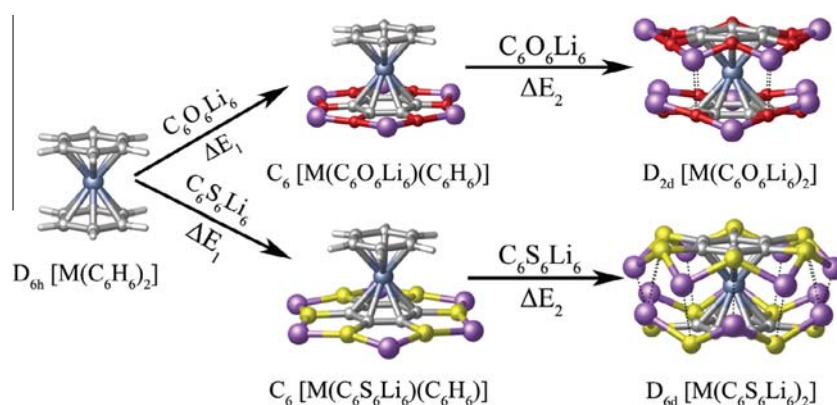
Fig. 4. Two-step ligand-exchange reactions of $M(C_6H_6)_2$ to produce $M(C_6X_6Li_6)_2$ (M = Cr, Mo, W; X = O, S).
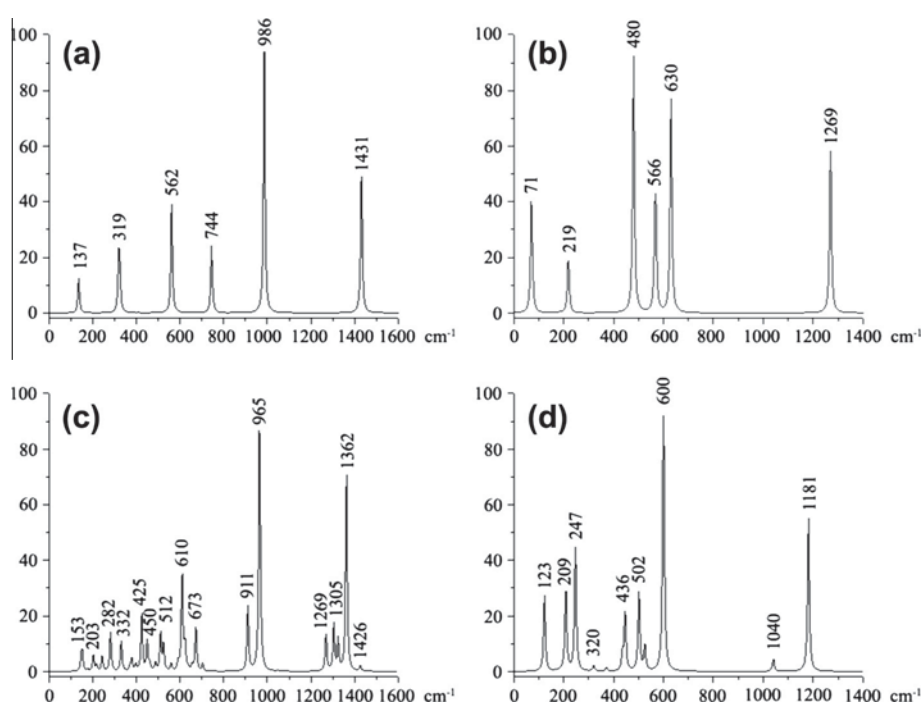
Fig. 5. Simulated IR spectra of D_{6h} $C_6O_6Li_6$ (a), $C_6S_6Li_6$ (b), D_{2d} $Cr(C_6O_6Li_6)_2$ (c), and $Cr(C_6S_6Li_6)_2$ (d) at B3LYP.

requires much more powerful computing capacities which are beyond the reach of available resources.

In order to further verify the stability of these sandwich complexes, we performed the first principle molecular dynamics (FPMD) simulations of $Cr(C_6O_6Li_6)_2$ and $Cr(C_6S_6Li_6)_2$ at 500 K for 10.0 ps at the B3LYP/6-31G* level. In both of the simulations, the covalent frameworks $Cr(C_6X_6)_2$ (X = O and S) maintained completely, while the Li^+ ions fluctuated around the covalent frameworks. Therefore, these sandwich complexes are stable in the high temperature.

In the surfaces of the sandwich complexes, there are many positive charged Li^+ ion (+0.73 to +0.86) and negative charged O atoms (-0.92 to -0.99, Table 1), so that these complexes can easily form the ionic dimmers. For instance, two D_{2d} $Cr(C_6O_6Li_6)_2$ sandwich units form two types of the stable $[Cr(Li_6C_6O_6)_2]_2$ dimmers: head-to-head and side-by-side (see Fig. S2), whose heats of formation from the monomers are -82.47 and -71.49 kcal/mol (including zero-point corrections), respectively. In both of the dimmers, the sandwich structures are perfectly maintained so that it is possible to further form the ionic crystals of these $M(C_6O_6Li_6)_2$ (M = Cr, Mo, W) units (see Fig. 4).

The predicted IR spectra of the sandwich complexes D_{2d} $Cr(C_6O_6Li_6)_2$ (c) and D_{6d} $Cr(C_6S_6Li_6)_2$ (d) compared with the ligands D_{6h} $C_6O_6Li_6$(a) and $C_6S_6Li_6$(b) are shown in Fig. 5. As seen from Fig. 5, the IR spectra of the high-symmetry D_{6h} $C_6O_6Li_6$ and $C_6S_6Li_6$ are relatively simple. The IR peak situate at 562 cm^{-1} in (a) and the strongest IR peak situate at 480 cm^{-1} in (b) correspond to the stretching vibration of O–Li and S–Li in $C_6O_6Li_6$ and $C_6S_6Li_6$ rings, respectively. The IR-peaks situate 137,319,744 cm^{-1} in (a) and 71,187,566 cm^{-1} in (b) correspond to the out-of-plane and in-plane C–X–Li bend vibrational resonances. The asymmetrical stretching vibrations of C–O bonds produce the IR absorption at 986 cm^{-1} for $C_6O_6Li_6$ and the stretching vibrations of C–S bonds produce two IR absorptions at 630 cm^{-1} for $C_6S_6Li_6$. Typical asymmetrical C–C stretching vibrations produce the IR absorptions at 1431 cm^{-1} and 1269 cm^{-1} for $C_6O_6Li_6$ and $C_6S_6Li_6$, respectively. The IR spectrum of the slightly distorted D_{2d} $Cr(C_6O_6Li_6)_2$ (c) and perfect D_{6d} $Cr(C_6S_6Li_6)_2$ (d) become complicated with the peaks located at 512 and 502 cm^{-1} for $C_6O_6Li_6$ and $C_6S_6Li_6$ corresponding to the characteristic asymmetrical breath vibrations of C–Cr bonds, which reveals the interactions between the transition-metal center and the ligands. The absorptions at 1269, 1040 cm^{-1} for

D_{2d} $Cr(C_6O_6Li_6)_2$ and D_{6d} $Cr(C_6S_6Li_6)_2$ corresponds to the asymmetrical stretching vibrations of C–C bonds, which corresponds the symmetrical breath vibrations of C–C in the free ligands. The peaks at 1362 and 1181 cm^{-1} corresponding to typical asymmetrical C–C stretching vibrations of $Cr(C_6O_6Li_6)_2$ and $Cr(C_6S_6Li_6)_2$ are apparently red-shifted compared with free $C_6X_6Li_6$(X = O, S) ligands (at 1431 and 1269 cm^{-1}, respectively), indicating that C–C bonds are slightly weakened with the formation of the sandwich complexes.

4. Summary

In summary, we have presented in this work strong theoretical evidences for the possible existence of the staggered sandwich complexes of $M(C_6X_6Li_6)_2$ (M = Cr, Mo, W; X = O, S). The d–π coordination bonds between transitional metal center and its ligands play the most important role in stabilizing these sandwich complexes. Detailed NICS and NICSzz analyses indicate that the $C_6X_6Li_6$ ligands in these sandwich complexes are aromatic in nature. These transition-metal sandwich complexes conforming to the 18-electron rule prove to be favored thermodynamically in theory and could be targeted in future experiments.

Acknowledgment

Appendix A. Supplementary material

Supplementary data associated with this article can be found, in the online version, at http://dx.doi.org/10.1016/j.comptc.2013.06.027.

References

[1] T.J. Kealy, P.L. Pauson, A new type of organo-iron compound, Nature 168 (1951) 1039–1040.
[2] S.A. Miller, J.A. Tebboth, J.F. Tremaine, Dicyclopentadienyliron, J. Chem. Soc. 114 (1952) 632–635.
[3] E.O. Fischer, W.Z. Hafner, Di-cyclopentadienyl-chrom (in German), Z. Naturforsch. B 8 (1953) 444–445.
[4] E.L. Muetterties, J.R. Bleeke, E.J. Wucherer, T.A. Albright, Structural, stereochemical, and electronic features of arene-metal complexes, Chem. Rev. 82 (1982) 499–525.
[5] R.B. King, Organometallic Syntheses. 1: Transition-Metal Compounds, Academic Press, New York, 1965.
[6] B.R. Sohnlein, D.S. Yang, Pulsed-field ionization electron spectroscopy of group 6 metal (Cr, Mo, and W) bis(benzene) sandwich complexes, J. Chem. Phys. 124 (2006) 134305.
[7] A.F. Neto, A.C. Pelegrino, V.A. Darin, Ferrocene: 50 years of transition metal organometallic chemistry-from organic and inorganic to supramolecular chemistry, Trends Organomet. Chem. 4 (2002) 147–169.
[8] S.D. Li, J.C. Guo, C.Q. Miao, G.M. Ren, [(η6-B6X)2M] (X=C, N; M=Mn, Fe, Co., Ni): a new class of transition-metal sandwich-type complexes, Angew. Chem. Int. Ed. 44 (2005) 2158–2161.
[9] S.D. Li, C.Q. Miao, G.M. Ren, J.C. Guo, Triple-decker transition-metal complexes $(C_nH_n)M(B_6C)M(C_nH_n)$ (M = Fe, Ru, Mn, Re; n = 5, 6) containing planar hexacoordinate carbon atoms, Eur. J. Inorg. Chem. (2006) 2567–2571.
[10] S.D. Li, C.Q. Miao, J.C. Guo, Tetradecker transition metal complexes containing double planar hexacoordinate carbons and double planar heptacoordinate borons, J. Phys. Chem. A 111 (2007) 12069–12071.
[11] E. Urnezius, W.W. Brennessel, C.J. Cramer, J.E. Ellis, P.v.R. Schleyer, A carbon-free sandwich complex $[(P_5)_2Ti]^{2-}$, Science 295 (2002) 832–834.
[12] R. Salcedo, Fullerenocene, Polyhedron 28 (2009) 431–436.
[13] K. Lee, H. Song, B. Kim, J.T. Park, S. Park, M.-G. Cho, The first fullerene-metal sandwich complex: an unusually strong electronic communication between two C_{60} cages, J. Am. Chem. Soc. 124 (2002) 2872–2873.
[14] X. Zhang, J. Wang, X. Zeng, Structural, electronic, and magnetic properties of $V_n(C_{60})_m$ complexes, J. Phys. Chem. A 113 (2009) 5406–5413.
[15] C.H. Wang, L.F. Xu, X.-L. Fan, J.-T. Wang, Structural stability and electronic property of sandwich clusters (CmHm)Mn(CnHn) (m, n = 5, 6) following an 18-electron principle, Phys. Lett. A 375 (2011) 562–567.
[16] S.D. Li, J.C. Guo, Planar tetracoordinate carbon atoms in M_4C square sheets (M = Ni, Pd, and Pt) sandwiched between the large π-coordinating ligands $[C_8H_8]^{2-}$ and $[C_9H_9]^-$, Eur. J. Inorg. Chem. (2010) 5156–5160.
[17] P. Jin, F. Li, Z. Chen, Theoretical design of novel trinuclear sandwich complexes with central M_3 triangles (M = Ni, Pd, Pt), J. Phys. Chem. A 115 (2011) 2402–2408.
[18] T.N. Gribanova, R.M. Minyaev, V.I. Minkin, Multi-decker tricarbonyl-bridged sandwich complexes of transition metals: structure, stability and electron-counting rules, Phys. Chem. Chem. Phys. 14 (2012) 14803–14809.
[19] K. Miyajima, S. Yabushita, M.B. Knickelbein, A. Nakajima, Stern−Gerlach experiments of one-dimensional metal−benzene sandwich clusters: Mn(C6H6)m (M = Al, Sc, Ti, and V), J. Am. Chem. Soc. 129 (2007) 8473–8480.
[20] G. Zhang, R. Zhou, Y. Gao, X.C. Zeng, Silicon-containing multidecker organometallic complexes and nanowires: a density functional theory study, J. Phys. Chem. Lett. 3 (2012) 151–156.
[21] H. Chen, M. Armand, G. Demailly, F. Dolhem, P. Poizot, J.-M. Tarascon, From biomass to a renewable $LixC_6O_6$ organic electrode for sustainable Li-ion batteries, ChemSusChem 4 (2008) 348–355.
[22] H. Chen, P. Poizot, F. Dolhem, N.I. Basir, O. Mentré, J.-M. Tarascon, Electrochemical reactivity of lithium chloranilate vs Li and crystal structures of the hydrated phases, Electrochem. Solid-State Lett. 12 (2009) A102–A106.
[23] M. Armand, S. Grugeon, H. Vezin, S. Laruelle, P. Ribiere, P. Poizot, J.-M. Tarascon, Conjugated dicarboxylate anodes for Li-ion batteries, Nat. Mater. 8 (2009) 120–125.
[24] D. Schröder, H. Schwarz, S. Dua, S.J. Blanksby, J.H. Bowie, Mass spectrometric studies of the oxocarbons C_nO_n (n=3–6), Int. J. Mass Spectrom 188 (1999) 17–25.
[25] R.B. Wyrwas, C.C. Jarrold, Production of $C_6O_6^-$ from oligomerization of CO on molybdenum anions, J. Am. Chem. Soc. 128 (2006) 13688–13689.
[26] X. Zhou, D.A. Hrovat, W.T. Borden, Calculations of the relative energies of the $^2B_{1g}$ and $^2A_{2u}$ states of cyclobutanetetraone radical cation and radical anion provide further evidence of a $^3B_{2u}$ ground state for the neutral molecule: a proposed experimental test of the prediction of a triplet ground state for $(CO)_4$, J. Phys. Chem. A 114 (2010) 1304–1308.
[27] J.-C. Guo, G.-L. Hou, S.-D. Li, X.-B. Wang, Probing the low-lying electronic states of cyclobutanetetraone (C_4O_4) and its radical anion: a low-temperature anion photoelectron spectroscopic approach, J. Phys. Chem. Lett. 3 (2012) 304–308.
[28] X.-G. Bao, X. Zhou, C.F. Lovitt, A. Venkatraman, D.A. Hrovat, R. Gleiter, R. Hoffmann, W.T. Borden, Molecular orbitals of the oxocarbons (CO)n, n = 2–6. Why does (CO)4 have a triplet ground state?, J Am. Chem. Soc. 134 (2012) 10259–10270.
[29] J.-C. Guo, H.-G. Lu, S.-D. Li, First-principles investigations on $C_5O_5^{-/0}$ and $C_6O_6^{-/0}$ oxocarbons, Comput. Theoret. Chem. 1007 (2013) 9–14.
[30] A.J. Fatiadi, W.F. Sager, Organic Syntheses 5 (1973) 595.
[31] A.M. Richter, V. Engels, N. Beye, E. Panghanel, Organiache elektronenleiter und vorstufen; znr darstellnng von hexa-natrium-benzenhexathiulat aus hexakis-benzylthio-benzen, Z. Chem. 29 (1989) 444–445.
[32] C.C. Wang, C.T. Kuo, P.T. Chou, G.H. Lee, The first rhodizonate metal complex with a novel 2D chair-like M_6 metal organic framework: $[M(C_6O_6)(bpym)(H_2O)]_nH_2O$ (M = Cd (1), n = 1; M = Mn (2), n = 2; bpym = 2,2'-bipyrimidine) and associated luminescence properties, Angew. Chem. Int. Ed. 4 (2004) 4507–4510.
[33] H.K. Yip, A. Schier, J. Riede, H. Schmidbaur, Benzenehexathiol as a template rim for a golden wheel: synthesis and structure of [{CSAu(PPh3)}6], J. Chem. Soc. Dalton Trans. (1994) 2333–2334.
[34] Z. Chen, L.R. Sutton, D. Moran, A. Hirsch, W. Thiel, P.v.R. Schleyer, A theoretical and structural investigation of thiocarbon anions, J. Org. Chem. 68 (2003) 8808–8814.
[35] H. Chen, M. Armand, M. Courty, M. Jiang, C.P. Grey, F. Dolhem, J.n-M. Tarascon, P. Poizot, Lithium salt of tetrahydroxybenzoquinone: toward the development of a sustainable Li-Ion battery, J. Am. Chem. Soc. 131 (2009) 8984–8988.
[36] E. Asato, A. Kyan, T. Madanbashi, T. Tamura, M. Tadokoro, M. Mizuno, The first example of metallocene-like coordination mode of $THBQ^{4-}$: a mixed-valence heptanucler palladium complex $[Pd_7(THBQ)_2(tben)_6](PF_6)_4$, Chem. Commun. 46 (2010) 1227–1228.
[37] M. Wu, J.D. Burton, E.Y. Tsymbal, X.C. Zeng, P. Jena, Multiferroic materials based on organic transition-metal molecular nanowires, J. Am. Chem. Soc. 134 (2012) 14423–14429.
[38] A.D. Beck, Density functional thermochemistry. III. The role of exact exchange, J. Chem. Phys. 98 (1993) 5648–5659.
[39] C. Lee, W. Yang, R.G. Parr, Development of the Colle-Salvetti correlation-energy formula into a functional of the electron density, Phys. Rev. B. 37 (1988) 785–791.
[40] J.P. Perdew, J.A.S. Chevary, H. Vosko, K.A. Jackson, M.R. Pederson, D.J. Singh, C. Fiolhais, Atoms, molecules, solids, and surfaces: applications of the generalized gradient approximation for exchange and correlation, Phys. Rev. B 46 (1992) 6671–6687.
[41] D. Feller, The role of databases in support of computational chemistry calculations, J. Comp. Chem. 17 (1996) 1571–1586.
[42] K.L. Schuchardt, B.T. Didier, T. Elsethagen, L. Sun, V. Gurumoorthi, J. Chase, J. Li, T.L. Windus, Basis set exchange: a community database for computational sciences, J. Chem. Inf. Model. 47 (2007) 1045–1052.
[43] J.M.L. Martin, A. Sundermann, Correlation consistent valence basis sets for use with the Stuttgart–Dresden–Bonn relativistic effective core potentials: the atoms Ga–Kr and In–Xe, J. Chem. Phys. 114 (2001) 3408–3420.

[44] P.v.R. Schleyer, C. Maerker, A. Dransfeld, H. Jiao, N.J.R.E. Hommes, Nucleus-independent chemical shifts: a simple and efficient aromaticity probe, J. Am. Chem. Soc. 118 (1996) 6317–6318.

[45] P.v.R. Schleyer, H. Jiao, N.J.R.E. Hommes, V.G. Malkin, O.L. Malkina, An evaluation of the aromaticity of inorganic rings: refined evidence from magnetic properties, J. Am. Chem. Soc. 119 (1997) 12669–12670.

[46] C. Corminboeuf, T. Heine, G. Seifert, P.v.R. Schleyer, Induced magnetic fields in aromatic [n]-annulenes – interpretation of NICS tensor components, Phys. Chem. Chem. Phys. 6 (2004) 273–276.

[47] A. Stanger, Nucleus-independent chemical shifts (NICS): distance dependence and revised criteria for aromaticity and antiaromaticity, J. Org. Chem. 71 (2006) 883–893.

[48] M.J. Frisch, G.W. Trucks, H.B. Schlegel, G.E. Scuseria, M.A. Robb, J.R. Cheeseman, J.A. Montgomery, Jr., T. Vreven, K.N. Kudin, J.C.Burant, J.M. Millam, S.S. Iyengar, J. Tomasi, V. Barone, B. Mennucci, M. Cossi, G. Scalmani, N. Rega, G.A. Petersson, H. Nakatsuji, M. Hada, M. Ehara, K. Toyota, R. Fukuda, J. Hasegawa, M. Ishida, T. Nakajima, Y. Honda, O. Kitao, H.Nakai, M. Klene, X. Li, J.E. Knox, H.P. Hratchian, J.B. Cross, C.Adamo, J. Jaramillo, R. Gomperts, R.E. Stratmann, O. Yazyev, A.J. Austin, R. Cammi, C. Pomelli, J.W. Ochterski, P.Y. Ayala, K. Morokuma, G.A. Voth, P. Salvador, J.J. Dannenberg, V.G.Zakrzewski, S. Dapprich, A.D. Daniels, M.C. Strain, O. Farkas, D.K. Malick, A.D. Rabuck, K. Raghavachari, J.B. Foresman, J.V. Ortiz, Q. Cui, A.G. Baboul, S. Clifford, J. Cioslowski, B.B. Stefanov, G. Liu, A. Liashenko, P. Piskorz, I. Komaromi, R.L. Martin, D.J. Fox, T. Keith, M.A. Al-Laham, C.Y. Peng, A. Nanayakkara, M. Challacombe, P.M.W. Gill, B. Johnson, W. Chen, M.W. Wong, C. Gonzalez, J.A. Pople, Gaussian 03, Revision B.03, Gaussian Inc., Pittsburgh, PA, 2003.

[49] CYLview, 1.0b, C.Y. Legault, Université de Sherbrooke, 2009. <http://www.cylview.org>.

[50] Molekel, version 5.4.0.8, U. Varetto, Swiss National Supercomputing Centre: Manno, Switzerland, 2009.